Journal of Hydrology 521 (2015) 170–181

Contents lists available at ScienceDirect

Journal of Hydrology

journal homepage: www.elsevier.com/locate/jhydrol

Understanding the low-frequency variability in hydroclimatic attributes over the southeastern US

Hui Wang [a,*], A. Sankarasubramanian [b], R.S. Ranjithan [b]

[a] The Bureau of Economic Geology, Jackson School of Geosciences, University of Texas at Austin, TX 78758, United States
[b] Civil, Construction and Environmental Engineering, North Carolina State University, Raleigh, NC 27695, United States

ARTICLE INFO

Article history:
Received 11 July 2014
Received in revised form 26 September 2014
Accepted 27 September 2014
Available online 22 November 2014
This manuscript was handled by Konstantine P. Georgakakos, Editor-in-Chief, with the assistance of Ercan Kahya, Associate Editor

Keywords:
Interannual variability
Decadal oscillations
Singular Spectrum Analysis
Basin storage effect
Water management

SUMMARY

Most studies on evaluating the potential in developing seasonal to interannual hydroclimatic forecasts have focused on associating low-frequency climatic conditions with basin-level precipitation/streamflow. The motivation of this study is to provide an understanding on how land surface characteristics modulate the low-frequency (interannual to decadal) variability in precipitation to develop low-frequency signal in streamflow. For this purpose, we consider basins with minimum anthropogenic impacts over southeastern United States and apply Singular Spectrum Analysis (SSA), a data-driven spectrum analysis tool, on annual precipitation and streamflow time series for detecting the dominant frequencies and for estimating the associated variability with them. Hypothesis test against an AR(1) process is carried out via Monte Carlo SSA for detecting significant (at 90% confidence level) low-frequency oscillations. Thus, the study investigates how the observed low-frequency oscillations in precipitation/streamflow vary over the southeastern United States and also their associations with climatic conditions. For most study basins, precipitation exhibits higher low-frequency oscillations than that of streamflow primarily due to reduction in variability by basin storage. Investigating this further, we found that the percentage variance accounted by low-frequency oscillations in streamflow being higher for larger basins which primarily indicates the increased role of climate and basin storage. To develop a fundamental understanding on how basin storage controls the low-frequency oscillations in streamflow, a simple annual hydrological model is employed to explore how the given low-frequency signal in precipitation being modified under different baseflow index conditions and groundwater residence time. Implications of these analyses relating to streamflow predictions and model calibration are also discussed.

1. Introduction

Detection and attribution of low-frequency oscillations in hydroclimatic data are of importance to understanding climate variability and their implications on water management. Understanding the association between low-frequency sea surface temperature (SST) conditions and local/regional hydroclimatology could also provide useful information for improving decadal hydroclimatic prediction. Contrary to the centenary-long span of typical climate projections, decadal climate predictions over the next 10–30 years have been gaining attention due to the interest in their relevance to supporting infrastructure planning and decision making. Meehl et al. (2009) discussed the challenges in decadal climate projections and suggested that reliable projections of climatic conditions such as El-Nino Southern Oscillations (ENSO) over the near-term (10–30 years) could significantly improve decadal climate projections. But, hydroclimatic variability at interannual to decadal time scales could be influenced by changing climatic signals as well as by land-surface characteristics. In this study, we investigate the role of basin storage in modulating the low-frequency variability in streamflow over the Southeast US (SEUS).

It is well documented in the hydroclimatic literature that climatic teleconnections such as ENSO influence regional precipitation and streamflow. Peel et al. (2002) investigated the variability of annual precipitation and its relation to El Niño-Southern Oscillation (ENSO) on global scale and concluded that the annual precipitation variability in ENSO-influenced continent is higher compared to continents that are not influenced by ENSO. Zeng (1999) studied the hydrological cycle in the Amazon basin and found that on interannual timescales the hydrologic variability in the atmosphere and at the land surface is closely related to ENSO. Westra and Sharma (2006) examined the relationship between

* Corresponding author. Tel.: +1 512 471 9299; fax: +1 512 471 0140.
E-mail address: watersystemresearch@gmail.com (H. Wang).

http://dx.doi.org/10.1016/j.jhydrol.2014.09.081
0022-1694/

ENSO and annual precipitation for 216 stations over Australia and found significant correlation between the two attributes over eastern Australia. Tootle et al. (2005) investigated the coupled oceanic–atmospheric variability and US streamflow. Their results show that in addition to the well-established ENSO signal the Pacific Decadal Oscillation (PDO), Atlantic Multidecadal Oscillation (AMO) and North Atlantic Oscillation (NAO) influence streamflow variability in the United States. Almanaseer and Sankarsubramanian (2012) also show that ENSO influences precipitation, temperature, streamflow and groundwater during the winter season over the Southeast US. Milly and Wetherald (2002) carried a theoretical study to investigate the effect of the land process on the runoff variability and found that groundwater and surface water storage could cause a strong reduction in low-frequency variability in many basins. Shun and Duffy (1999) detected and analyzed low-frequency oscillations in precipitation, temperature and runoff for a mountain watershed in Utah and concluded that low-frequency oscillation in streamflow could be introduced by groundwater storage alone even if precipitation does not exhibit any oscillatory behavior.

Most of the above studies could be grouped into two categories: (a) dependency analyses between ENSO index and the hydroclimatic attributes using correlation or similar measures (Peel et al., 2002; Tootle et al., 2005; Almanaseer and Sankarsubramanian, 2012), and (b) spectral analyses on streamflow for identifying low-frequency components (Shun and Duffy, 1999; Milly and Wetherald, 2002). This study, on the other hand, performs detailed spectral analyses using Singular Spectrum Analyses (SSA) both for identifying the periodic components on the hydroclimatic attributes – precipitation and streamflow – and for quantifying and comparing the percentage variance explained by the interannual and interdecadal components in the hydroclimatic attributes. By comparing the percentage variance explained by low frequency components in streamflow and precipitation, we quantify the role of land surface storage in modulating/enhancing the low-frequency components in precipitation. Further, the study also explores how land-surface storage itself alone could modulate/enhance low-frequency variability in streamflow in the absence/presence of low-frequency components in the forcings – precipitation and potential evapotranspiration – using a conceptual water balance model.

The main intent of this paper was to: (1) systematically decompose the observed hydroclimatic variability based on long time series of precipitation and streamflow into low-frequency components at interannual and interdecadal time scales; and (2) to understand how those components are modulated due to storage and basin characteristics over the SEUS. Given the significant correlation between El Niño-Southern Oscillation (ENSO) and precipitation variability over the SEUS (Ropelewski and Halpert, 1987; Almanaseer and Sankarsubramanian, 2012), it is natural to expect similar low-frequency oscillatory components in streamflow over many watersheds in the region. However, streamflow variability does not depend only on the local precipitation variability and exogenous climatic variability (e.g., ENSO), but also on the basin storage and watershed characteristics. For this purpose, we have assembled long time series of precipitation and streamflow over these 56 basins in the SEUS (Table 1). There are different approaches for frequency analysis, e.g., Multi-taper spectral analysis (Lall and Mann, 1995; Mann et al., 1995; Rajagopalan et al., 1998), wavelet analysis (Sang, 2013) and Singular Spectrum Analysis (SSA). We employ a data driven approach, Singular Spectrum Analysis (SSA) to detect the low-frequency oscillations in precipitation and streamflow. There are three advantages of SSA: (1) it is data driven in the sense that one does not have to assume its data structure; (2) its simplicity for use; and (3) its robustness in separating noise from low-frequency signals by employing Monte Carlo SSA, which is discussed in the methodology section. We further compare the variability explained by the respective components in each variable to explain the role of land-surface storage in modulating/introducing low-frequency components in streamflow for the selected watersheds over the SEUS.

The paper is organized as follows: Section 2 provides a brief description of data set and the SSA methodology. Results from the SSA and the diagnostic analyses using a conceptual water

Table 1
Basin drainage area and data length of precipitation and streamflow time series of the 56 selected basins over SEUS in this study.

Station ID	USGS gage (starting year)	Area (Km^2)	Station ID	USGS gage (starting year)	Area (Km^2)
1	02045500(1931)	579	29	02296750(1932)	1367
2	02051500(1930)	552	30	02298830(1937)	229
3	02061500(1938)	320	31	02301500(1933)	335
4	02070000(1937)	108	32	02313000(1932)	1825
5	02074500(1930)	112	33	02314500(1938)	1260
6	02083000(1927)	526	34	02317500(1933)	1400
7	02083500(1932)	2183	35	02320500(1932)	7880
8	02085500(1926)	149	36	02321500(1932)	575
9	02102000(1931)	1434	37	02322500(1933)	1017
10	02126000(1930)	1372	38	02329000(1927)	1140
11	02132000(1930)	1030	39	02347500(1938)	1850
12	02134500(1930)	1228	40	02349500(1931)	2900
13	02136000(1930)	1252	41	02358000(1929)	17200
14	02138500(1923)	66.7	42	02361000(1936)	686
15	02154500(1931)	116	43	02369000(1939)	474
16	02156500(1939)	2790	44	02371500(1938)	500
17	02198000(1938)	646	45	02374500(1938)	176
18	02202500(1938)	2650	46	02375500(1935)	3817
19	02203000(1938)	555	47	02387500(1894)	1602
20	02225500(1938)	1110	48	02392000(1937)	613
21	02226000(1932)	13600	49	02398000(1938)	192
22	02226500(1938)	1200	50	02448000(1939)	768
23	02228000(1931)	2790	51	02450000(1929)	365
24	02231000(1927)	700	52	02467000(1929)	15385
25	02232500(1934)	1539	53	02472500(1939)	304
26	02236000(1934)	3066	54	02475500(1939)	369
27	02246000(1932)	177	55	02479000(1931)	6590
28	02256500(1932)	311	56	02488500(1939)	4993

balance model are presented in Section 3, which is followed by discussion in Section 4. Finally, we draw the major findings and conclusion from the study in Section 5.

2. Hydroclimatic databases and SSA methodology

This section provides detailed information on the annual time series of precipitation, temperature and streamflow over 56 HCDN watersheds in the SEUS. Fig. 1 provides an overview of the performed analyses in the study.

2.1. Annual hydroclimatic data and climate indices (step 1 in Fig. 1)

Given that our focus is to explain inter-annual and inter-decadal variability in hydroclimatic attributes over the SEUS, we assembled long time series of annual precipitation and streamflow from 56 stations with at least 70 years of observed records (Table 1). All the selected basins are chosen from Hydro-climatic Dataset Network (HCDN) (Slack et al., 1993a,b), which consists of the observed streamflow from basins that are not impacted by pumping storage. The importance of HCDN basins in understanding large-scale hydroclimatology is discussed well in the literature (Martinez and Gupta, 2010; Sankarasubramanian and Vogel, 2002). These stations are spread over seven states with drainage area varying from 229 square miles to 17,200 square miles. Annual streamflow data are obtained from the historical database from USGS. Since the previous hydroclimatic database archived at Oak Ridge National Laboratory (Vogel and Sankarasubramanian, 2005) has the monthly data till 1990, we extended that database till 2010 by spatially averaging the precipitation and temperature for the selected basins by using the Parameter-elevation Regressions on Independent Slopes Model (PRISM) gridded database. PRISM is a knowledge-based system that uses point measurements to produce continuous, digital grid estimates of climatic parameters (Daly et al., 1994) with a spatial resolution of 4 Km × 4 Km. Monthly minimum and maximum temperature and extraterrestrial solar radiation (Dingman, 2008) were used to estimate monthly time series of potential evapotranspiration (PET) with Hargreaves method (Hargreaves and Samani, 1985). Monthly precipitation and PET were aggregated to obtain annual time series of precipitation and PET. Monthly minimum and maximum temperature were averaged over the year to obtain average annual temperature for a given year.

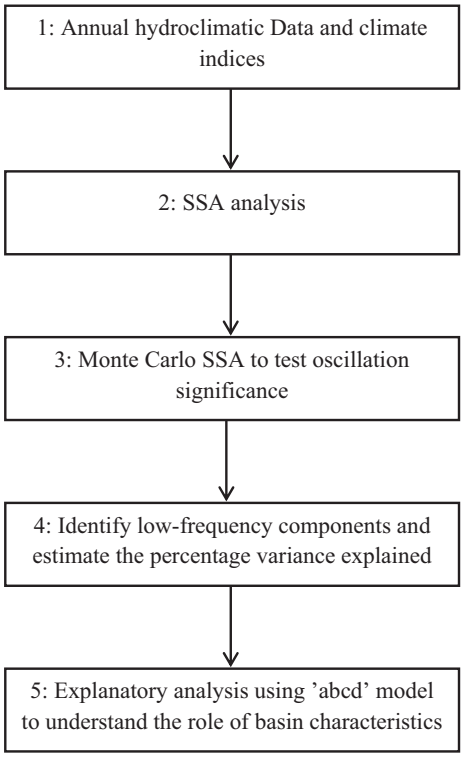

Fig. 1. An overview of the performed analysis in this study. Step 1 to Step 4 is SSA of streamflow and precipitation data, while step 5 is explanatory analysis to understand the role of basin characteristics in modulating oscillations in streamflow.

In addition to hydroclimatic data, we also obtain climatic indices, e.g., ENSO index. ENSO refers to the natural coupled cycle in the ocean–atmospheric system over the tropical Pacific. It is characterized by variations in the temperature of the surface of the tropical eastern Pacific Ocean and air surface pressure over the tropical Pacific. Warm and cold phases of ENSO have been found to be associated with regional and global climate variability as well as streamflow variability (Ropelewski and Halpert, 1987; Piechota et al., 1997). Studies have shown that the ENSO is the only driver in influencing annual precipitation over the continental US (Quan et al., 2006; Devineni and Sankarasubramanian, 2010a,b). For this study, we consider monthly Nino-3.4 index; which reflects the Sea Surface Temperature (SST) anomaly over the region bounded by 120W–170W and 5S-5 N. Monthly Nino 3.4 indices were obtained from International Research Institute for Climate and Society (http://portal.iri.columbia.edu) and they were annually averaged for further analysis.

2.2. Singular Spectrum Analysis – description (steps 2–4 in Fig. 1)

To investigate the frequency associated with the annual time series of precipitation and streamflow, we employed Singular Spectrum Analysis (SSA) (Ghil et al., 2002). SSA is demonstrated as a useful approach for both frequency analysis and dimension reduction of short, noisy time series. A detailed review of the SSA technique from the perspective of the evolution of a nonlinear dynamic system is provided by Ghil et al. (2002). One advantage of SSA is that no assumption of the data structure is made beforehand. It has been further developed since then and has extensive application in geospatial data analysis (Dettinger et al., 1995; Shun and Duffy, 1999; Kumar and Duffy, 2009). Decomposition and reconstruction of a time series are the two complementary processes of SSA (Elsner and Tsonis, 1996). We briefly describe the SSA methodology below. For additional details, see Ghil et al. (2002).

Consider a real valued time series $X = (x_0, x_1, \ldots, x_N)$ with length $N > 2$. By choosing an embedding dimension m, SSA forms $j = N - m + 1$ lagged vectors

$$X_j = (x_{j-1}, x_j, \ldots, x_{j+m-2})^T \quad j = 1, 2, \ldots, N - m + 1; \tag{1}$$

The trajectory matrix of X is

$$W = [X_1, X_2, \ldots, X_j]; \tag{2}$$

The covariate matrix S is defined as

$$S = W * W^t \tag{3}$$

Upon completion of decomposition, a series of eigenvalues $(\lambda_1, \lambda_2, \ldots, \lambda_m)$ and eigenvectors $(V_1, V_2, \ldots, V_m)$ of S will be obtained. The corresponding eigenvalue is proportional to variation explained by the reconstructed component from the eigenvector. A pair of eigenvalues of about the same magnitude corresponds to a certain oscillation/periodicity, which provides the basis for frequency analysis based on eigenvectors.

A hypothesis test is used to decide whether the detected oscillations are significant or not. Eigenvalues do not follow a specific distribution; hence, analytical derivation of confidence intervals on eigenvector is not available. Allen and Smith (1996) discussed a robust approach to carry out hypothesis test using nonparametric techniques. They suggested that an AR(1) process, a stochastic process can be modeled as a first order autoregressive model that specifies the output variable depends on its own previous values, is an appropriate null hypothesis since it does not support oscillations. Monte Carlo SSA is used to estimate parameters for an AR(1) process and then generate random realizations from the estimated AR(1) process. For each realization, eigenvalues corresponding to the same frequency are chosen to construct the confidence interval. After initial investigation, we choose 1000 Monte Carlo simulations of AR(1) process in the null hypothesis test to obtain the 90% confidence interval on the eigenvalues. Length of annual streamflow dataset is between 70 and 80; therefore, the chosen embedding dimension is 25. As for annual precipitation, the embedding dimension is 35 since the length of dataset is 110 (from year 1900 to 2009). Besides component decomposition, it is easy to reconstruct time series based on identified oscillations. Component reconstruction essentially adds up identified oscillations from original time series and interested readers are referred to Elsner and Tsonis (1996).

In this study, SSA is applied to find the dominant and significant low-frequency components associated with hydroclimatic datasets and corresponding percentages of variability explained by the quasi-periodic oscillations (step 2). Monte Carlo SSA of annual precipitation and annual streamflow for each basin is carried out independently (step 3) to ensure whether the identified components are statistically significant (Allen and Smith, 1996; Matalas and Sankarasubramanian, 2003). Oscillations with periodicity between 3 and 7 years are characterized as interannual signal, while oscillations with periodicity higher than 8 years are defined as decadal oscillations (step 4). Dependency between low-frequency oscillations in hydroclimatic datasets and oceanic–atmospheric indices is also investigated to relate/identify the source of variability. The role of basin characteristics including drainage area is considered to explain the spatial variability in the percentage variance accounted by the significant low-frequency components. Differences in the estimated low-frequencies on precipitation and streamflow are compared to analyze how storage dampens the periodicity in precipitation.

2.3. Explanatory analysis – "abcd" model description (step 5 in Fig. 1)

Given that SSA over 56 watersheds exhibited different combinations of interannual and decadal components on precipitation and streamflow, we employ a conceptual water balance model over selected watersheds to understand what values of basin characteristics could result in such different scenarios of low-frequency components on streamflow. One could consider the conceptual water balance model as a stochastic filter that dampens/enhances the observed low-frequency signal in precipitation in modulating the low-frequency signal on streamflow.

The "*abcd*" model is a physical-based, nonlinear conceptual water balance model, which was original introduced by Thomas (1981). Detailed description of this model is omitted here and interested readers are referred to Thomas (1981) and Vogel and Sankarasubramanian (2003). The underground is divided into two layers, of which the upper layer is unsaturated and the lower layer is the saturated zone. In each of the two zones, part of water mass is retained as soil moisture in upper layer and groundwater in saturated zone. Meanwhile, upper and lower zone contributes to surface streamflow in the form of direct runoff and baseflow, respectively. There are only four parameters introduced in this model to control mass balance. Parameter a reflects the propensity of runoff to occur before the soil is fully saturated (Thomas, 1981) and it is between 0 and 1. Urbanization and deforestation, as expected, tend to decrease the value of a. In this paper, all 56 basins are selected from HCDN dataset where there is minimum degree of anthropogenic influences; hence, a is close to 1. Parameter b is defined as the upper limit on the sum of actual evapotranspiration and soil moisture. It represents the maximum storage in the unsaturated zone above the ground water and quantifies the ability of the basin to hold water within the unsaturated zone. The higher value of b, the higher resulting soil moisture storage. Parameter c, baseflow index, is usually defined as the ratio of the groundwater outflow over the streamflow. It controls the allocation of the available water in the unsaturated zone. A certain amount of water percolates into the groundwater and the remaining flows out as direct runoff. The reciprocal of parameter d is the average groundwater residence time.

In our explanatory analysis, parameters a and b are fixed to their calibrated values, while different combinations of parameters c and d are used to simulate different realizations of streamflow and groundwater. SSA is then applied to simulate streamflow and groundwater data.

3. Results

3.1. SSA results for precipitation and streamflow data

To begin with, we first show the eigen spectrum of SSA a representative basin (USGS#02479000) where interannual and decadal oscillations exist in both annual precipitation and streamflow data (Fig. 2). A pair of similar eigen values that are both higher than 90% confidence interval of the corresponding frequency is identified as significant oscillations. There are two pairs of identified oscillations shown in Fig. 2(a) and (c) for precipitation and streamflow, respectively. Fig. 2(b) and (d) shows the ranked eigen values in precipitation and streamflow data for the representative basin. It is important to note that oscillation frequency exhibiting in hydrological attributes is the reciprocal of oscillation period. For instance, if the identified frequency is 0.1 cycle/year, then corresponding period is 10 years.

We extended the above analyses for all the 56 watersheds. Based on this, we found four different combinations of oscillations in precipitation and streamflow data (Table 2). As we believe 3–7 year oscillations are related to ENSO, we use ENSO-related oscillations and 3–7 year quasi-periodic oscillation exchange ably. In the first category, ENSO-related oscillations are identified in both precipitation and streamflow time series, e.g., the representative basin in Fig. 2 In the second category, no oscillation is found in streamflow data while ENSO-related oscillations are found in precipitation data .In the third category, both ENSO-related and decadal oscillations are identified in precipitation and streamflow data. In the last category, only decadal oscillations are found in streamflow while both ENSO-related and decadal oscillations are detected in precipitation data. Based on Table 2, we found that 3–7 year quasi-periodic oscillations exist in both precipitation and streamflow data for 43 basins. For four basins, we found 3–7 year oscillations in precipitation but no oscillatory components in the annual streamflow. Similar observation is valid for another 5 basins where no 3–7 year oscillations are detected in streamflow data. It is clear from Table 2 that quasi-periodic oscillations found in precipitation might be modulated by basin storage and soil characteristics since the periodicity of the detected oscillations is usually lesser in streamflow. This will be examined later using a water balance model.

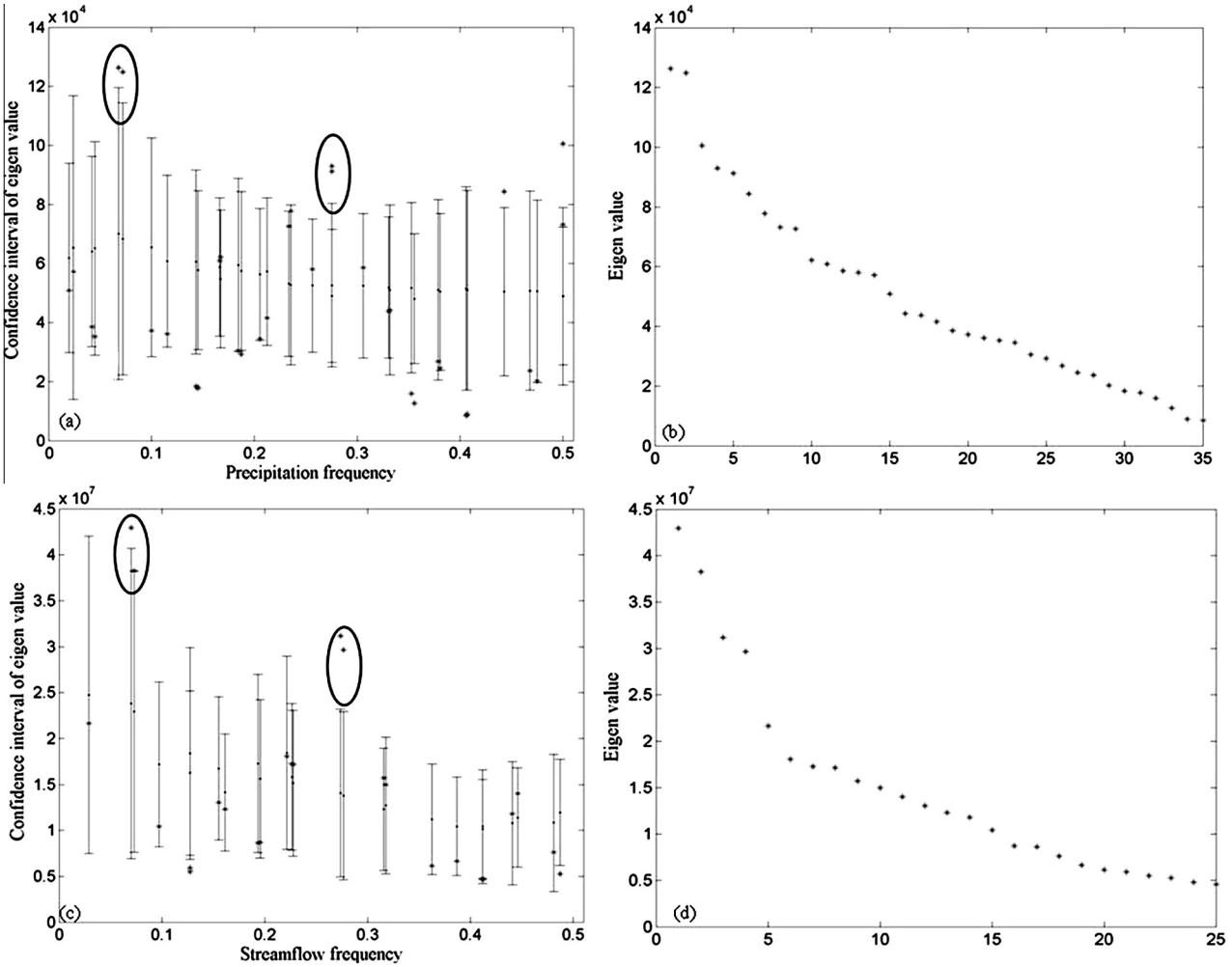

Fig. 2. SSA for precipitation and streamflow data at station 55 (USGS #02479000). (a) Confidence interval of eigen values from Monte Carlo SSA, as well as calculated eigen value (represented as stars) from covariate matrix of precipitation data. The eigen values included in the circles are identified frequencies exhibited in the dataset. (b) Eigen spectrum of covariate matrix of annual precipitation. (c) Confidence interval of eigen values from Monte Carlo SSA, as well as calculated eigen value (represented as stars) from covariate matrix of streamflow data. (d) Eigen spectrum of covariate matrix of annual streamflow.

Table 2
Four different combinations of quasi-periodic oscillations in precipitation and streamflow considered from the data analysis. Number of stations falling in each category is listed and the number in the bracket denotes the station index chosen for further exploratory analysis.

Streamflow	Precipitation			
	ENSO-related	Decadal	ENSO-Decadal	None
ENSO-related	**43**(13)			
Decadal			**5**(45)	
ENSO-Decadal			**4**(55)	
None	**4**(40)			

The bold number is the ID of a representative basin for each category.

To further examine the difference in the pattern of quasi-periodic oscillations in precipitation and streamflow, we calculated the ratio of the percentage variance explained by the quasi-periodic 3–7 year component in annual streamflow to the percentage variance explained by the 3–7 year quasi-periodic components in annual precipitation, defined as α, which is shown in Fig. 3. Ratio greater than one indicates higher portion of annual streamflow could be explained by the 3–7 year oscillatory component as opposed to the precipitation. It is important to note that quasi-periodic components are selected only if it is statistically significant under AR(1) null hypothesis. The ratio, α, is greater than 1 for 33 basins, among which it is greater than 2 for six basins. This denotes that the 3–7 year oscillatory components explain a large percentage of variability in streamflow than that in precipitation for those basins.

Similar information is shown in Fig. 4(a), where the diagonal 45 degree line divides all the 56 basins into two categories: $\alpha >= 1$ and $\alpha < 1$. For the basins above (below) the diagonal line, quasi-periodic oscillations are enhanced (reduced) in annual streamflow from those exhibited in annual precipitation. Nine basins do not exhibit 3–7-year quasi-periodic oscillations in streamflow. For those exhibiting quasi-periodic oscillations in streamflow, the variability explained by periodic-oscillations ranges from 5% to 40%.

To understand the role of basin scale in quantifying the percentage variance explained (3–7 year components) in streamflow, we plot the percentage variance in streamflow as a function of drainage area (Fig. 4b). As shown in Fig. 4b, the plot clearly reveals a positive correlation indicating larger basins with increased storage account for higher percentage variance based on the 3–7 year periodic component. The rank correlation between the two attributes is 0.40, which is statistically significant at the 0.05 significance level. Hence, oscillations in streamflow have been modulated/amplified by the land-surface characteristics of the basin and groundwater storage.

To understand whether the variability accounted in 3–7 year oscillatory components in precipitation and streamflow could be

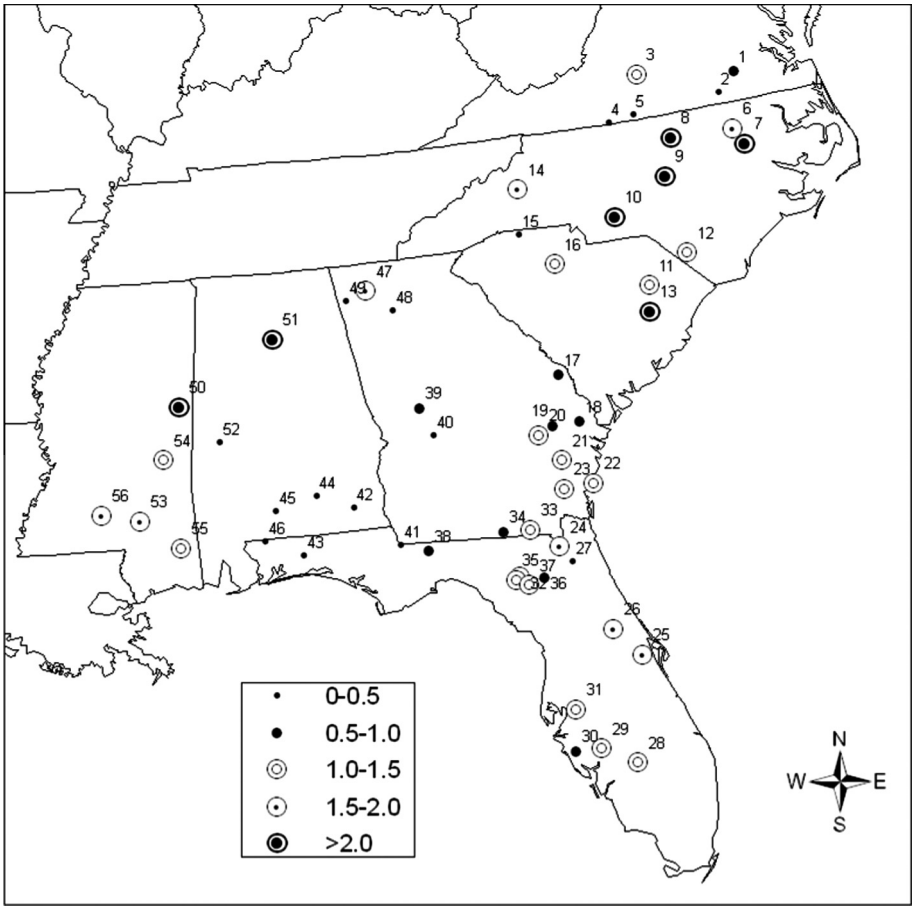

Fig. 3. Ratio of the percentage variance explained by the quasi-periodic (3–7 years) components in streamflow to the percentage variance explained by the 3–7 year quasi-periodic components in precipitation. The number next to the stations indicates station index shown in Table 1.

associated with ENSO, we computed rank correlation between annual streamflow/precipitation and the NINO3.4 index. It is well-known that precipitation and streamflow are influenced by ENSO over the Southern United States especially during the winter season. Fig. 4a shows that both precipitation and streamflow have statistically significant correlation with Nino 3.4 index in 22 basins out of the selected 56 basins indicating the role of ENSO on both hydroclimatic attributes. For five basins, precipitation alone has statistically significant correlation with the Nino 3.4 index. In this context, the watershed acts as a low-cut filter with the residence time of groundwater being higher than the ENSO time scale. Only one basin (station 11) exhibits significant correlation between streamflow and ENSO with the basin precipitation having no significant correlation with ENSO.

To analyze the same information exclusively from ENSO perspective, we obtain the reconstructed precipitation and streamflow time series using the components whose eigen values are significant over ENSO bandwidth (3–7 years). Fig. 5b shows the scatterplot of rank correlation between the reconstructed 3–7 year oscillatory components in precipitation (R^P_{3-7}) and Nino 3.4 index and the rank correlation between the reconstructed 3–7 year oscillatory components in streamflow (R^Q_{3-7}) and Nino 3.4 index. A striking difference between Fig. 5a and b is that the correlation between reconstructed 3–7 year oscillatory component streamflow and Nino 3.4 is significant for additional nine basins (shown as squares in Fig. 5b) while the correlation between the observed annual streamflow and Nino 3.4 for those basins is not significant. For instance, the correlation between 3 and 7 year reconstructed components in streamflow and Nino 3.4 is 0.40 for basin 33, while the observed streamflow is not correlated with Nino 3.4. Even though for these nine basins, 3–7 year reconstructed streamflow component and Nino 3.4 are significant, given that the annual precipitation does not exhibit any relation with ENSO, the low-frequency signal that we see in streamflow could be induced purely by groundwater storage. This is similar to the findings of Shun and Duffy (1999) who found groundwater storage alone could induce low-frequency components that are at ENSO time scale. Thus, to distill the information from Fig. 5, basin storage primarily resulting from increased groundwater residence time could act as a low-cut filter in removing the low-frequency signal from precipitation (Fig. 5a – triangles) and basin storage alone could induce a low-frequency signal in streamflow at ENSO time scale (squares in Fig. 5a and b).

To further examine the role of basin storage in modulating the low-frequency oscillatory components in precipitation, dominant frequencies exhibited in both precipitation and streamflow are compared (Fig. 6). The striking information from Fig. 6 is that the periodicity in streamflow is always equal/lesser than the periodicity in precipitation. For those reside on or nearby the 45 degree line, the frequencies exhibited in precipitation and streamflow are about the same. This denotes that oscillatory components in precipitation and streamflow have the same period, although the percentage of variability explained by those low-frequency components could be completely different. For most of the basins, we find that the frequencies exhibited in precipitation are higher than those in streamflow indicating the low-frequency signal is being dampened by the basin storage indicating watershed acts as a low-cut filter.

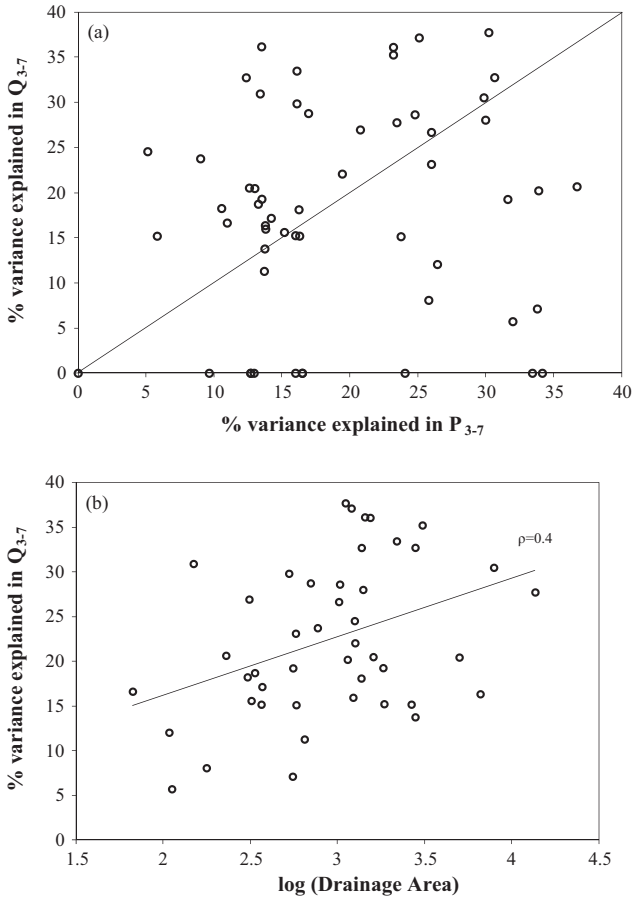

Fig. 4. (a) Scatter-plot of percentage of variance explained by quasi-periodic components in precipitation and streamflow. (b) Scatter-plot of percentage of variance explained by the 3–7 year oscillatory components in streamflow and logarithm drainage area.

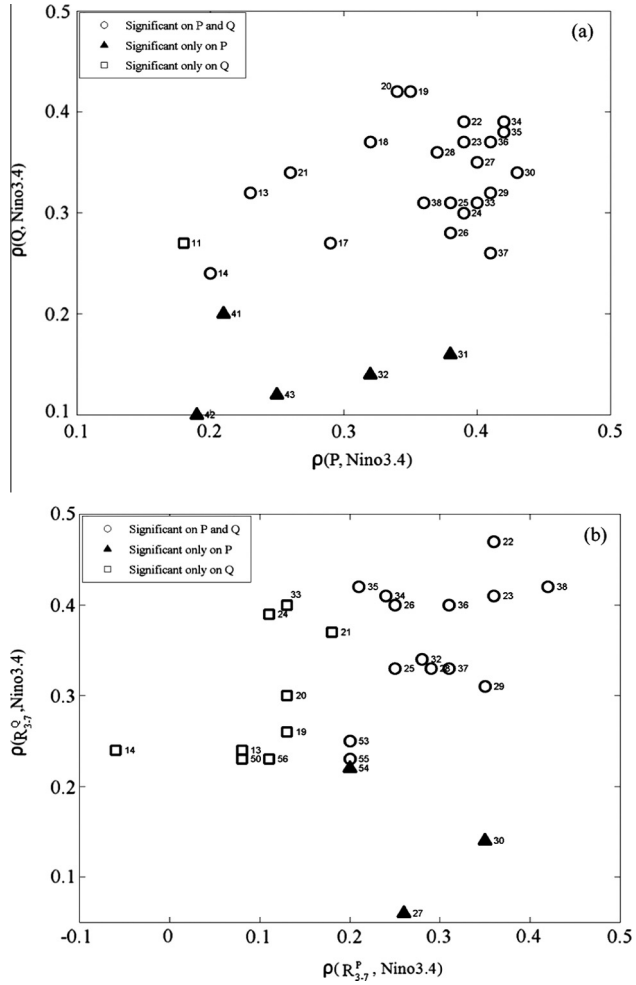

Fig. 5. Rank correlation between precipitation/streamflow and Nino 3.4 index, as well as rank correlation between oscillatory components in precipitation/streamflow and Nino 3.4 index is calculated for all 56 basins. Only statistically significant correlations are shown in the figure. (a) Scatterplot of $\rho_{P,Nino3.4}$ and $\rho_{Q,Nino3.4}$, where $\rho_{P,Nino3.4}$ denotes correlation between annual precipitation and Nino 3.4; $\rho_{Q,Nino3.4}$ denotes correlation between annual streamflow and Nino 3.4. (b) Scatterplot of rank correlation between Nino 3.4 and R^Q_{3-7} and rank correlation between Nino 3.4 and R^P_{3-7}, where R^Q_{3-7} is (reconstructed) oscillatory components with 3–7 year period in streamflow data and R^P_{3-7} is (reconstructed) oscillatory components with 3–7 year period in precipitation data. Note that basin ID is shown aside by the symbols.

Longer periods exhibited in streamflow data reflect the modulation of basin characteristics including the land-surface processes and groundwater. If the variances explained by precipitation and streamflow are similar for a given quasi-periodic component, we would expect that basin characteristics, such as groundwater storage, do not modulate, indicating that the residence time of groundwater is exactly as that of the frequency of the quasi-periodic component. It is hence important to examine whether any possible oscillations exhibited in groundwater data. Limited groundwater data in the study area prevented thorough analysis of frequencies exhibited in groundwater. Two streamflow gages with nearby groundwater wells are identified. One is Flint River in Georgia (USGS#02347500) and the other is Tar River in North Carolina (USGS#02083500). Fig. 7 shows groundwater level at Tar River basin and the identified quasi-period component. The oscillatory component has frequency 0.28 per year and it explains 43% of the variances exhibited in the annual groundwater data at this location. Quasi-periodic oscillations explain 16.1% and 33.45% of variances in precipitation and streamflow data for this site. Oscillations exhibited in groundwater might be one of the reasons that lead to enhanced variance explained by quasi-period component in streamflow data. Similar analysis was conducted for groundwater data in the Flint River basin. Though it has a relatively long record of 59 years, no significant oscillations were identified. This is consistent with the fact that the variance explained by the quasi-periodic oscillations is very similar for precipitation and streamflow at this site, i.e., 16.0% and 15.2%, respectively.

3.2. Exploratory analyses using "abcd" water balance model

To overcome the data limitation of groundwater, "*abcd*" model is used to simulate groundwater content, as a surrogate to groundwater depth. The purpose of this exploratory analysis using "*abcd*" model is to understand how different combinations of baseflow index (parameter "*c*") – fraction of groundwater in streamflow – and groundwater residence time (inverse of parameter "*d*") could control/modulate the low-frequency signal in streamflow. We assume the parameter "*a*" – inclination to produce overland runoff – and parameter "*b*" – analogous to soil moisture holding capacity– will exhibit frequencies at intra-annual time scale with limited/no influence on inducing low frequency signal in streamflow. Hence, we just considered the calibrated parameters for "*a*" and "*b*" to obtain the simulated streamflow under different sets of "*c*" and "*d*".

Fig. 8a shows the comparison of annual streamflow observation and simulated streamflow for basin 7 (USGS#02083500). The Spearman correlation between the two is 0.85, which is

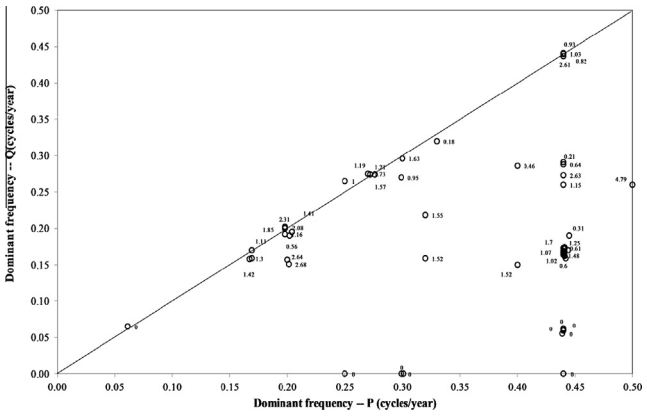

Fig. 6. Comparison of statistically significant frequencies exhibited in precipitation and streamflow data. The labels represent the ratio of the percentage variance explained by the quasi-periodic (3–7 years) components in streamflow to the percentage variance explained by the 3–7 year quasi-periodic components in precipitation.

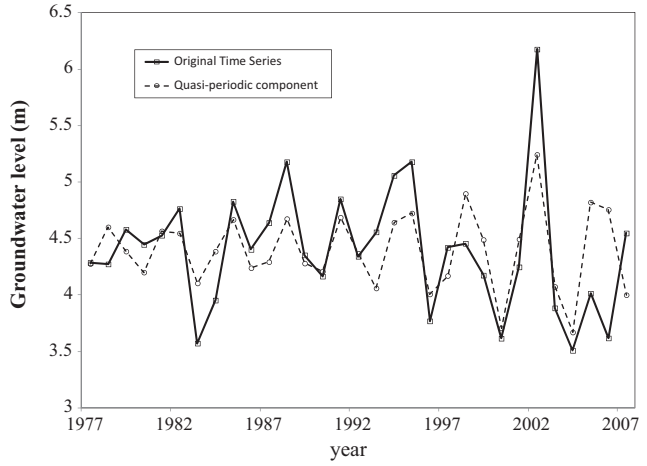

Fig. 7. SSA of groundwater level at station index 7 (USGS #02083500). The dashed line represents quasi-periodic component with frequency of 0.28/year explaining about 43% of the variances in the annual groundwater data.

statistically significant at the 0.05 significance level. Mean Absolute Error (MAE) of the simulated streamflow is less than 5% of average annual flow. Fig. 8b shows the scatterplot of groundwater table depth and simulated groundwater variable. The trend line represents a correlation of −0.54 between the two variables, which is also statistically significant at the 0.05 significance level. This denotes that simulated groundwater from "*abcd*" model is a sufficient surrogate for groundwater depth in frequency analysis due to the scarcity of long term record of groundwater observation.

Four basins, each representing a relationship between the quasi-period oscillation in precipitation and streamflow data shown in Table 2, are identified to carry exploratory analysis using the "*abcd*" model and Monte Carlo SSA. The selected basin index and calibrated parameter values, as well as Spearman correlation between simulated streamflow and observation are shown in Table 3.

As discussed earlier, parameters *a* and *b* are fixed to their calibrated values in conducting exploratory analysis, while different combinations of parameter *c* and *d* are used to simulate different realizations of streamflow and groundwater. The range for both parameters *c* and *d* is from 0 to 1. For each set of model parameters,

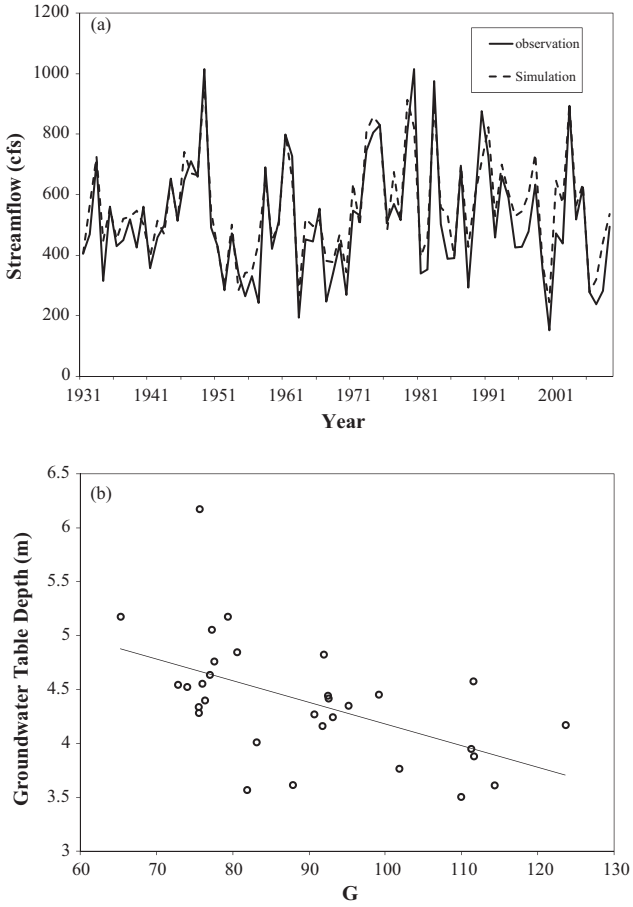

Fig. 8. Panel (a) shows that "*abcd*" model simulated annual streamflow fits well with the observation (USGS#02083500). Panel (b) shows simulated ground water depth, *G*, (mm/year) and the observed groundwater levels from the surface.

Monte Carlo SSA is carried on simulated streamflow and groundwater data. Results from the four representative basins are discussed as follows.

3.2.1. Case 1

In case 1, ENSO-related oscillations present in both precipitation and streamflow data. For the selected basin 13 (USGS#02136000), ENSO-related oscillations are detected in both precipitation and streamflow data, with frequency 0.4 per year in precipitation data and 0.24 per year in streamflow data. Reconstructed oscillatory components in streamflow explain about 24% of the total variances of streamflow and oscillatory components in precipitation account for 5.12% of variance exhibited in annual precipitation data. Fig. 9a shows the possible oscillations that would be detected under different combinations of parameters *c* and *d*. The yellow triangle denotes the values for calibrated parameters *c* and *d*, which are 0.08 and 0.72 respectively. The contour lines represent the percentage of variance being explained by the detected oscillation. It can be seen that ENSO-related oscillations are detected when *c* is less than 0.4. By examining the location of the calibrated parameters, the oscillatory components explain 20–25% variance of the simulated time series, which is in line with the analysis from the observed time series (24%). When parameter *c* is greater than 0.4, no significant oscillatory components are detected in simulated streamflow data. Monte Carlo SSA is also carried for simulated groundwater time series under different combinations of parameters *c* and *d*, but no oscillatory component is detected for this site. This indicates increased recharge ($c > 0.4$)

Table 3
Calibrated parameter values and Spearman correlation between the observed streamflow and the calibrated streamflow from "*abcd*" model for selected basins.

Station index	*a*	*b*	*c*	*d*	ρ
13	0.99	1244	0.08	0.72	0.768
40	0.98	1560.6	0.70	0.76	0.785
45	0.98	1444.34	0.58	0.13	0.962
55	0.98	1700.1	0.11	0.12	0.857

could result in removal of low-frequency components with the groundwater modulating at the annual time scale.

3.2.2. Case 2

For the selected basin 40 (USGS#02349500), ENSO-related oscillations are detected in precipitation while no oscillation exhibits in streamflow. Oscillatory components in precipitation account for 16% of the total variance. Fig. 9b shows the oscillation category detected in potential annual streamflow under various combinations of parameters *c* and *d*. It can be seen that no oscillatory components detected when *c* is greater than 0.6. It is important to note that the calibrated parameters lie in the area where no oscillatory components are exhibited by the streamflow. The contour lines denote that a very small percentage of variance is explained by oscillation when *c* is greater than 0.4. In observed streamflow data, no oscillatory components are detected and this is in line with potential streamflow time series, corresponding to the location of the calibrated parameters *c* and *d* denoted by the yellow triangle. Similar to case 1, no significant oscillatory components are detected in groundwater data.

3.2.3. Case 3

For the selected basin 45 (USGS#02374500), there are ENSO-related and decadal oscillations in precipitation time series but only decadal oscillation is detected in streamflow data. Oscillatory components explain 16% of variance exhibited in precipitation. Fig. 10a depicts the oscillatory components at ENSO or decadal time scale as well as the percentage of variance explained by these oscillations. Similar to cases 1 and 2, there are no oscillations when the value of *c* is relatively large ($c > 0.8$) and d is relatively small ($d < 0.5$). Under such circumstance, the ENSO-related oscillations can be filtered by the basin storage; hence, they do not exist in simulated streamflow data. The location of the calibrated parameters *c* and *d* corresponding to only decadal time scale oscillations can be detected in simulated streamflow data, which is in line with the oscillations detected in observed streamflow time series.

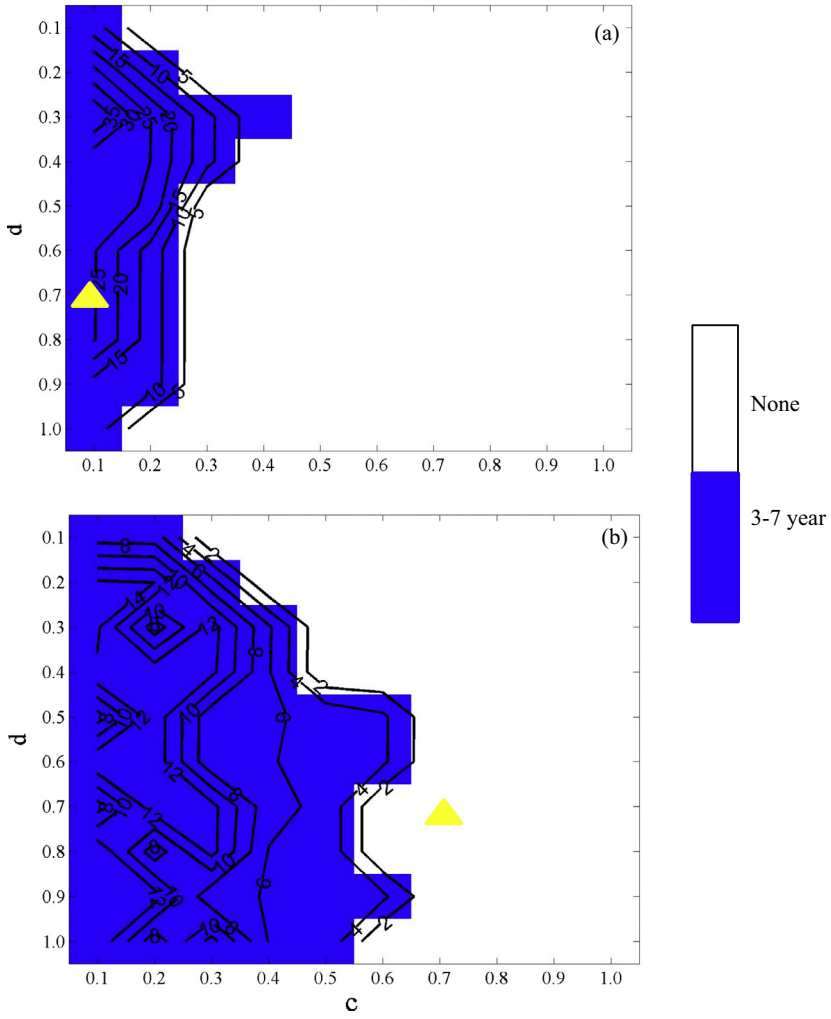

Fig. 9. SSA of "*abcd*" model simulated streamflow for station index 13 (USGS#02136000) (a) and for station index 40 (USGS#02349500) (b) under different parameter values of "*c*" and "*d*". The contour represents the percentage of variance explained by quasi-periodic components in streamflow. The yellow triangle represents the calibrated values of "*c*" and "*d*" parameters. (For interpretation of the references to color in this figure legend, the reader is referred to the web version of this article.)

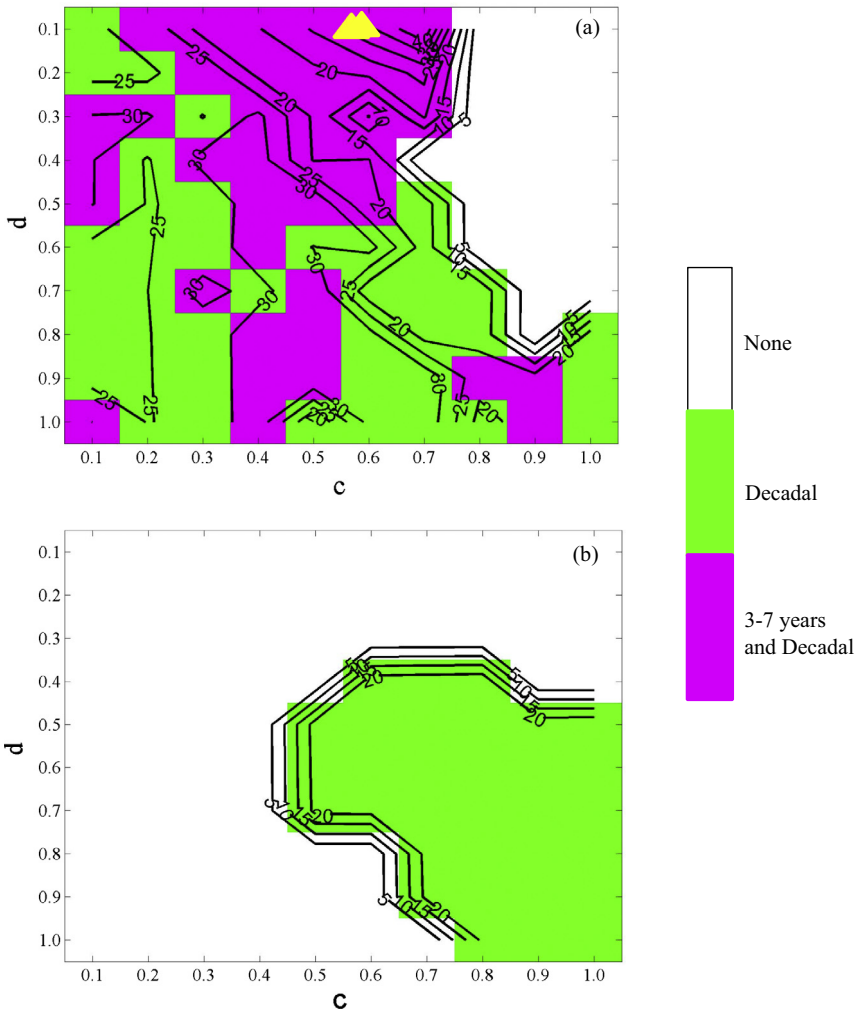

Fig. 10. SSA of "*abcd*" model simulated streamflow (a) and groundwater (b) for station 45 (USGS#02374500). The contour represents the percentage of variance explained by quasi-periodic components in streamflow. The yellow triangle represents the calibrated values of "*c*" and "*d*" parameters. (For interpretation of the references to color in this figure legend, the reader is referred to the web version of this article.)

As shown in Fig. 10b, when the value of parameters *c* and *d* is relatively large ($c > 0.7$ and $d > 0.5$), decadal oscillatory components are detected in simulated groundwater time series. This can be, in part, explained by the reasoning that signal in precipitation is carried to groundwater since a large portion of precipitation contributes to groundwater. At the same time, a small *d* value denotes increased residence time of groundwater. Hence, decadal signal remains in groundwater. It is important to note that 3–7 year periodic oscillations are not detected in streamflow data while calibrated model suggests that simulated streamflow contains such low-frequency components. This denotes that our model calibration can be improved upon this and it is a separate research question beyond the scope of this paper. We have provided relevant discussion in Section 4.

3.2.4. Case 4

For the selected basin 55 (USGS#02479000), ENSO-related and decadal oscillations are detected in both precipitation and streamflow time series. Among the four representative basins, basin 55 illustrates the most comprehensive case where there are all possible oscillations exhibiting in simulated streamflow data, as shown in Fig. 11a. Under certain circumstances, both the decadal and ENSO time scale oscillations in precipitation are exhibiting in streamflow data.

Similar to basin 45, when the value of parameters *c* and *d* is relatively large ($c > 0.5$ and $d > 0.5$), decadal oscillatory components are detected in simulated groundwater time series. Compared to basin 45, the percentage of variance explained by oscillatory components in groundwater data is larger in basin 55. This is probably due to the reason that the drainage area of basin 55 is much larger than that of basin 45; therefore, it has a stronger "memory" accounting for increased variance. In summary, land-surface characteristics and basin storage play a significant role in modifying the quasi-periodic oscillations exhibited in precipitation. Application of SSA on precipitation and streamflow reflects the following information: (1) ENSO associated low-frequency information present in precipitation could be entirely filtered by the basin storage (Fig. 5a); (2) Low-frequency signal at ENSO bandwidth could be entirely generated by the groundwater storage alone (Fig. 5b); (3) Dominant frequency in streamflow is the same as or lesser than that exhibited in precipitation (Fig. 6); and (4) Percentage of variance explained by oscillatory components in streamflow is usually higher than that explained by oscillatory components in precipitation (Fig. 4). Hence, both the low frequency and the associated magnitude of the oscillations exhibited in precipitation could be modulated by the basin storage leading to reduced/no low frequency oscillations with potentially increased variance associated with those oscillations. This led to an exploratory study using a

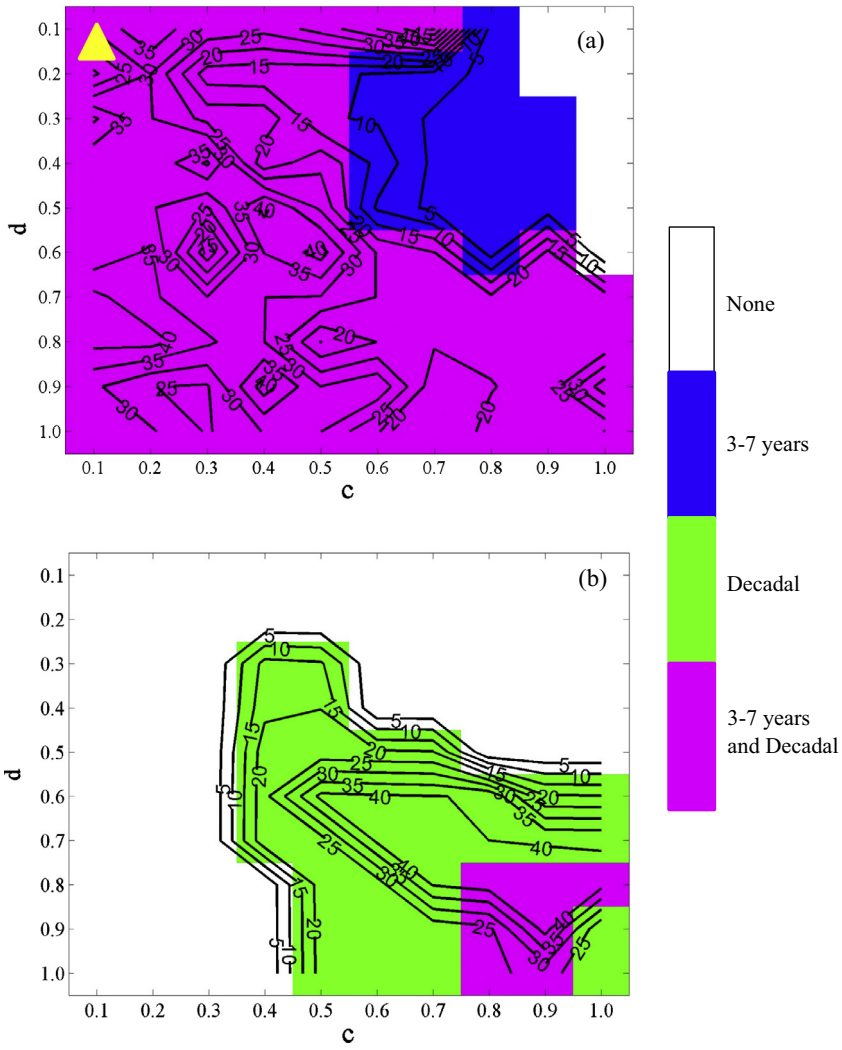

Fig. 11. SSA of "*abcd*" model simulated streamflow (a) and groundwater (b) for basin 55 (USGS#02479000). The contour represents the percentage of variance explained by quasi-periodic components in streamflow. The yellow triangle represents the calibrated values of "*c*" and "*d*" parameters. (For interpretation of the references to color in this figure legend, the reader is referred to the web version of this article.)

watershed model investigating the four types of relationship between oscillations exhibited in precipitation and streamflow that indicates how both baseflow index (parameter "*c*") and groundwater residence time (parameter "*d*") influence the oscillatory components in streamflow. Results clearly show that different combination of parameters *c* and *d* could lead to varying oscillations in streamflow and groundwater (see case 4 as an example). Note that basin drainage area, which often indicates the size of groundwater storage, plays an important role in modulating oscillations from precipitation.

4. Discussion

Exploratory analysis using the "*abcd*" model (Figs. 9–11) shows that in few cases simulated streamflow with the calibrated parameters does not preserve the observed low-frequency oscillations in streamflow. This emphasizes the findings from earlier studies that calibrating the watershed models was purely based on minimizing the sum of squares of errors between observed and validated streamflow do not provide validation of the model in estimating the observed moments (Vogel and Sankarasubramanian, 2003). Validation of a watershed model by evaluating its ability to preserve the observed moments and periodicity is critical in employing the application of the watershed model. This study adds additional emphasis on the findings of Vogel and Sankarasubramanian (2003) that it is important to validate the watershed model by evaluating its ability to reproduce the observed moments and low-frequency oscillations in observed streamflow. Perhaps, calibration of the watershed model should consider optimization strategies that preserve the moments and low-frequency oscillations in the observed streamflow. Pauwels and De Lannoy (2011) discussed model calibration in frequency domain and demonstrated that it is of the same skill as model calibration in time domain. To examine whether calibrated model can preserve the oscillations in streamflow could be one more metric to consider in model calibration. Further research is required in substantiating the applicability of these strategies in model calibration.

Findings from this study also have implications in developing low-dimensional statistical models for streamflow forecasting. For instance, one could develop a low-dimensional model between streamflow and Nino3.4 for basins that have significant correlations between streamflow and Nino3.4 alone (Fig. 5). In fact, the exhibited low-frequency signal purely arises from groundwater storage since there is no dependency between precipitation and

Nino3.4. Another interesting aspect that emerges from the study is the separation of observed streamflow into quasi-periodic oscillations and non-oscillatory components. One could associate the low-frequency components of precipitation/streamflow with the low-frequency components of climatic indices (e.g., Nino3.4) to estimate the moisture transport from outside the basin/region. Non-oscillatory components could be associated with the in-basin storage, which could be estimated by associating the non-oscillatory components of groundwater levels and tree rings. A manuscript based on this separation technique for streamflow reconstruction for eight basins over the southeastern US is currently under review (Patskoski et al., submitted for publication). Thus, the fundamental understanding developed in this study on how basin storage modulates the low-frequency signal in streamflow has potential applications on both streamflow forecasting and reconstruction.

5. Conclusion

In this study, SSA, a data driven approach, is applied to detect possible quasi-periodic oscillations, interannual and interdecadal time scales, in annual precipitation and streamflow data in SEUS at 90% confidence level. Low-frequency oscillatory components (3–7 years on the ENSO bandwidth) on the hydroclimatic attributes are significantly correlated with teleconnections, e.g., ENSO index, especially for those basins in coastal areas. This indicates that low-frequency oscillations in exogenous climatic conditions could be a potential source of quasi-periodic oscillations in precipitation and streamflow data. The percentage of variance explained by quasi-periodic oscillations in streamflow is highly correlated with the logarithm of drainage area indicating the role of basin storage. Observed low-flow frequency components in the precipitation is modulated significantly by the basin storage resulting in reduced low-frequency signal in the observed streamflow. We also observed that in a few basins, groundwater storage alone can generate low-frequency signal in streamflow even though the basin precipitation did not exhibit any low-frequency oscillatory components. Exploratory analysis is further carried out to examine the role of basin storage, baseflow index and groundwater residence time, in inducing the low-frequency oscillations in streamflow. Analyses also show that in a few watersheds the simulated streamflows obtained using the calibrated parameters from the "*abcd*" watershed model did not preserve the low-frequency oscillations in the observed streamflow indicating the need for developing calibration strategies which preserve the observed low-frequency signals in hydroclimatic attributes.

Acknowledgments

The work was supported by Award #0756269 from the Environmental Sustainability Program of the National Science Foundation (NSF). Any opinions, findings and conclusion expressed in this materials are those of the authors and do not necessarily reflect the views of NSF. The authors thank the anonymous reviewers for their thoughtful and critical comments that improved the manuscript.

References

Allen, M.R., Smith, L.A., 1996. Monte Carlo SSA: detecting irregular oscillations in the presence of colored noise. J. Clim. 12 (9), 3373–3404.
Almanaseer, N., Sankarsubramanian, A., 2012. Role of climatic variability in modulating the surface water and groundwater interaction over southeast US. J. Hydrol. Eng. 17 (9), 1001–1010.
Daly, C., Neilson, R.P., Philips, D.L., 1994. A statistical-topographic model for mapping climatological precipitation over mountainous terrain. J. Appl. Meteorol. 33 (2), 140–158.
Dettinger, M.D., Ghil, M., Keppenne, C.L., 1995. Interannual and interdecadal variability in United States surfact-air temperatures, 1910–87. Clim. Change 31, 35–66.
Devineni, N., Sankarasubramanian, A., 2010a. Improving the prediction of winter precipitation and temperature over the continental United States: role of ENSO state in developing multimodel combinations. Mon. Weather Rev. 138 (6), 2447–2468.
Devineni, N., Sankarasubramanian, A., 2010b. Improved categorical winter precipitation forecasts through multimodel combinations of coupled GCMs. Geophys. Res. Lett., 37.
Dingman, S.L., 2008. Physical Hydrology, second ed. Waveland Press Inc.
Elsner, J.B., Tsonis, A.A., 1996. Singular Spectrum Analysis, A New Tool in Time Series Analysis. Plenum Press, New York and London.
Ghil, M. et al., 2002. Advanced spectral methods for climatic time series. Rev. Geophys. 40 (1), 1003. http://dx.doi.org/10.1029/2000RG000092.
Hargreaves, G.H., Samani, Z.A., 1985. Reference crop evapotranspiration from temperature. Trans. ASAE 1 (2), 96–99.
Kumar, M., Duffy, C.J., 2009. Detecting hydroclimatic change using spatio-temporal analysis of time series in Colorado River Basin. J. Hydrol. 374, 1–15.
Lall, U., Mann, M., 1995. The Great Salt Lake: A barometer of low-frequency climatic variability. Water Resour. Res. 31 (10), 2503–2515.
Mann, M.E., Lall, U., Saltzman, B., 1995. Decadal-to-centennial-scale climate variability: Insights into the rise and fall of the Great Salt Lake. Geophys. Res. Lett. 22 (8), 937–940.
Martinez, G.F., Gupta, H.V., 2010. Toward improved identification of hydrological models: a diagnostic evaluation of the "*abcd*" monthly water balance model for the conterminous United States. Water Resour. Res. 46, W08507. http://dx.doi.org/10.1029/2009WR008294.
Matalas, N.C., Sankarasubramanian, A., 2003. Effect of persistence on trend detection via regression. Water Resour. Res. 39 (12), art.no.1342.
Meehl, G.A. et al., 2009. Decadal prediction. Bull. Am. Meterol. Soc. 90 (10), 1467–1485. http://dx.doi.org/10.1175/2009BAMS2778.1.
Milly, P.C.D., Wetherald, R.T., 2002. Macroscale water fluxes 3. Effects of land processes on variability of river discharge. Water Resour. Res. 38 (11), 1235. http://dx.doi.org/10.1029/2001WR000761.
Patskoski, J., Sankarasubramanian, A., Wang, H. Reconstructing streamflow in the Southeastern United States using SST and tree ring chronologies. Water Resour. Res. (submitted for publication).
Pauwels, V.R.N., De Lannoy, G.G.M., 2011. Multivariate calibration of a water and energy balance model in the spectral domain. Water Resour. Res. 47, W07523. http://dx.doi.org/10.1029/2010WR010292.
Peel, M.C., McMahon, T.A., Finlayson, B.L., 2002. Variability of annual precipitation and its relation to El Nino-Southern oscillation. J. Clim. 15 (3), 545–551.
Piechota, T.C., Dracup, J.A., Chiew, F.H.S., McMahon, T.A., 1997. Seasonal streamflow forecasting in eastern Australia and the El Niño –southern oscillation. Water Resour. Res. 34, 3035–3044.
Quan, X., Hoerling, M., Whitaker, J., Bates, G., Xu, T., 2006. Diagnosing sources of U.S. seasonal forecast skill. J. Clim. 19, 3279–3293. http://dx.doi.org/10.1175/JCLI3789.1.
Rajagopalan, B., Mann, M.E., Lall, U., 1998. A multivariate frequency-domain approach to long-lead climatic forecasting. Weather Forecast. 13, 58–74.
Ropelewski, C.F., Halpert, M.S., 1987. Global and regional scale precipitation patterns associated with the El Niño/Southern oscillation. Mon. Weather Rev. 115, 1606–1626.
Sang, Y.-F., 2013. A review on the applications of wavelet transform in hydrology time series analysis. Atmos. Res. 122, 8–15.
Sankarasubramanian, A., Vogel, R.M., 2002. Annual hydroclimatology of the United Sates. Water Resour. Res. 38 (6), art. no. 1083.
Shun, T., Duffy, C.J., 1999. Low-frequency oscillations in precipitation, temperature, and runoff on a west facing mountain front: a hydrogeologic interpretation. Water Resour. Res. 35 (1), 191–201.
Slack, J.R., Lumb, A.M., Landwehr, J.M., 1993a. Hydroclimatic data network (HCDN): A U.S. Geological Survey streamflow data set for the United States for the study of climate variation, 1874–1988. Water Resour. Invest. Rep., 93–4076.
Slack, J.R., Lumb, A., Landwehr, J.M., 1993b. Hydro-Climatic Data Network (HCDN) Streamflow Data Set, 1874-1998. CD-ROM. U.S. Geological Survey, Reston, Virginia, U.S.A. Available from Oak Ridge National Laboratory Distributed Active Archive Center, Oak Ridge, Tennessee, U.S.A. <http://www.daac.ornl.gov>.
Thomas, H.A., 1981. Improved Methods for National Water Assessment: Final Report, U.S. Geol. Water Resour. Contract WR15249270, 44pp.
Tootle, G.A., Piechota, T.C., Singh, A., 2005. Coupled oceanic–atmospheric variability and U.S. streamflow. Water Resour. Res. 41, W12408. http://dx.doi.org/10.1029/2005WR004381.
Vogel, R.M., Sankarasubramanian, A., 2003. The validation of a watershed model without calibration. Water Resour. Res. 39 (10), art.no.1292.
Vogel, R.M., Sankarasubramanian, A., 2005. USGS Hydro-Climatic Data Network (HCDN): Monthly Climate Database, 1951-1990, Data Set Available On-line from Oak Ridge National Laboratory Distributed Active Archive Center, Oak Ridge, Tennessee, USA. http://dx.doi.org/10.3334/ORNLDAAC/810.
Westra, S., Sharma, A., 2006. Dominant modes of interannual variability in Australian rainfall analyzed using wavelets. J. Geophys. Res. 111, D05102. http://dx.doi.org/10.1029/2005JD005996.
Zeng, N., 1999. Seasonal cycle and interannual variability in the Amazon hydrological cycle. J. Geophys. Res. 104 (D8), 9097–9106.